Tribological characteristics of bulk ($\overline{2}01$) β-Ga₂O₃ substrate crystals grown by EFG

P.N. Butenko [ID] [1], M.E. Boiko [ID] [1], A.V. Chikiryaka [ID] [1], L.I. Guzilova [ID] [1],

A.O. Pozdnyakov [1], M.D. Sharkov [ID] [1], A.V. Almaev [ID] [2], V.I. Nikolaev [ID] [1]

[1] Ioffe Institute, St. Petersburg, Russia

[2] Tomsk State University, Tomsk, Russia

✉ pavel.butenko@mail.ioffe.ru

Abstract. The tribological and mechanical tests of bulk substate crystals of gallium oxide β-polymorph grown by the EFG technique were carried out. The correlation of coefficient of friction and wear coefficient with hardness is discussed. It is shown that the smooth, epi-ready surface of ($\overline{2}01$) Ga₂O₃ samples has an extremely low resistance to abrasion by a sapphire ball. At the same time, the surface of the β-Ga₂O₃ wafer that has not undergone a complete post-growth processing cycle has high mechanical properties. It is pointed out that this difference can be due to deformation defects, which are entered into the subsurface layers during the mechanical impact on the semiconductor material.
Keywords: gallium oxide; EFG; wear; coefficient of friction; tribology; bulk crystals

Citation: Butenko PN, Boiko ME, Chikiryaka AV, Guzilova LI, Pozdnyakov AO, Sharkov MD, Almaev AV, Nikolaev VI. Tribological characteristics of bulk ($\overline{2}01$) β-Ga₂O₃ substrate crystals grown by EFG. *Materials Physics and Mechanics.* 2023;51(5): 153-161. DOI: 10.18149/MPM.5152023_15.

Introduction

Gallium oxide is one of the most promising ultra-wide bandgap semiconductor material. The monoclinic β-modification is the only Gallic phase obtained so far in a bulk form [1]. It attracts general attention of researchers. Currently, it is already used in electronics, such as MOS structures [2], and as a material for substrates [3].

An important factor that may constrain the expansion of Ga₂O₃ applications is the insufficient study of its mechanical properties. In particular, the resistance of this material to such an important impact as a friction has not been investigated thoroughly. Moreover, there are a limited number of publications analyzing the structure of mechanically deformable gallium oxide samples [4−18]. There are even fewer works, in which the mechanical characteristics of gallium oxide, determined by experimental or computational methods, appear [4–8,11–16,18]. At the same time, commercial semiconductor substrates produced from bulk Ga₂O₃ crystals are available. They are mechanically post-growth processed to obtain *epi-ready* surfaces for epitaxial growth for microelectronic applications [19,20]. A number of laboratories grow epitaxial films of the most common gallium oxide polymorphs, which can be applied as protective and functional coatings [21–23]. There are numerous

works devoted to the use of Ga_2O_3 as sensors [24–26], in these applications the material often operates at high temperatures and pressures. Such impacts are able to generate structure defects and cause internal stresses in crystals [9,10,17]. In all these cases, it is important to understand which changes occur in the surface structure and subsurface layers upon the specified effects, whether it is post-growth processing or direct operation.

In this work, the tribological characteristics of the semiconductor substrates produced from bulk β-Ga_2O_3 crystals grown by edge-defined film-fed growth (EFG) were measured. The results were correlated with the hardness of the surfaces undergone post-growth processing.

Materials and Methods

The bulk β-Ga_2O_3 commercial wafer produced by *Tamura Corp* using EFG technology was investigated. The samples in a form of single-crystal ($\bar{2}01$) plates of 5×6 mm and 650 μm thick were cut off from the wafer by a producer. For a chosen sample, one of it's ($\bar{2}01$) surfaces (referred to as "the bulk face" here and after) was chemically-mechanically polished (CMP) to make it applicable for epitaxial growth. The opposite surface (referred to as "the bulk back" here and after) was also subjected to post-growth treatment but having performed only a part of the processing cycle that terminates by polishing.

For the samples surface visualization, the Nikon Eclipse E200 was employed. The samples relief was studied with scanning electron microscopy (SEM) at *Phenom ProX* using secondary electron (SE) mode. The profiles of the sample surfaces and the roughness values were registered by *MarSurf PS-10* profilometer.

For a tribological experiment *AntonPaar TRB* tribometer was applied, employing reciprocating test, dry friction scheme and sphere-on-plane geometry. For all the samples ($\bar{2}01$) oriented surfaces were studied. To reduce the influence of gallium oxide anisotropy, which a changes its properties depending on the direction [27], the probe-run direction was set at 45º to the [100] direction of both types of surfaces. The tests were processed at fixed probe load, the 4mm diameter sapphire ball was applied as the counterbody. The coefficient of friction (COF) *(μ)* values were measured by the tribometer.

The wear coefficients (*k*) were calculated based on wear track geometry that was measured by the profilometer. The Archard model [28] was employed, which uses the following equation: $k = \dfrac{V}{F_n \cdot d}$, where *V* is the material volume that is removed during a tribotest, F_n is the probe load, *d* is the total probe run during a tribotest. For a more detailed description, see [16].

The phase composition of the samples was determined by X-ray diffraction (XRD) technique. The XRD data were registered at Bourevestnik DRON-6 laboratory device with the Cu K_α radiation ($\lambda = 1.5406$ Å) in a standard Bragg-Brentano configuration in the θ-2θ mode within the range of angles from 10 to 130 deg.

The hardness of the samples was studied by *LOMO PMT-3* hardness tester equipped with Vickers type indenter, *Axio Vert.A1* optical microscope and *Carl Zeiss Axiocam 208* color digital optical system. With its help, the geometrical parameters of the indent imprints were measured and the hardness values H_V were calculated. All the experiments were performed in standard conditions (NTP) at air relative humidity of 40 % RH.

Results and Discussion

Relief of the initial surfaces. SEM images of the initial β-Ga_2O_3 sample surfaces are shown in Fig. 1. The surface (bulk face) morphology of the sample which was subjected to CMP (Fig. 1(a)) is homogeneous and has no visible relief features in the scale presented. The

morphology of the polished surface (Fig. 1(b)) has a pronounced texture along a single direction due to the mechanical action (polishing without CMP).

To identify surface irregularities in depth, cross-sections were scanned in a plane perpendicular to the surface of the sample. The profiles and corresponding optical images are shown in Fig. 2. In both cases, the surface profiles are uniform and have no significant heterogeneity. The roughness values of the surfaces were determined and amounted as: R_a (bulk face) = 6 nm, R_a (bulk back) = 164 nm.
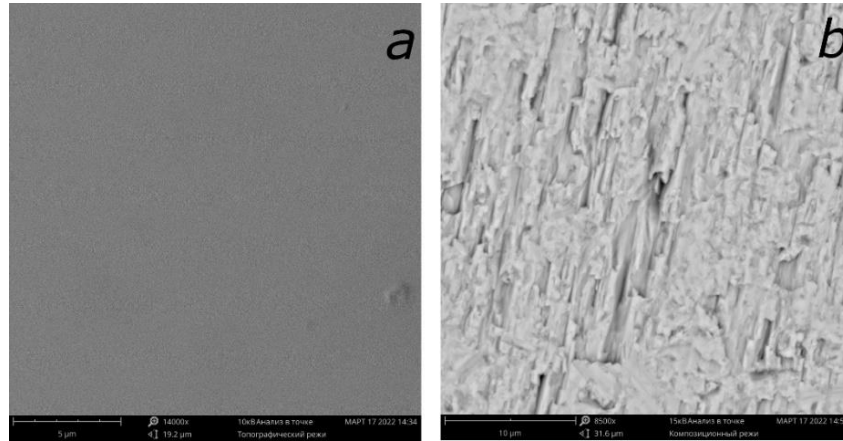

Fig. 1. SEM images of the initial surfaces of the β-Ga$_2$O$_3$ surface: bulk face (a), bulk back (b)
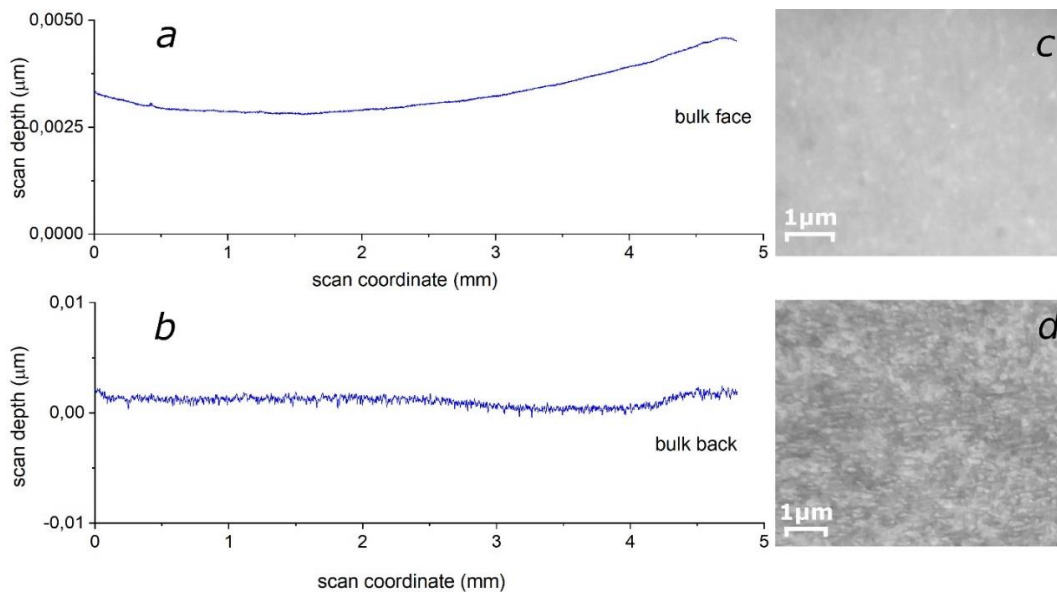

Fig. 2. The profiles and corresponding optical images the β-Ga$_2$O$_3$ surface: bulk face (a) and (c), bulk back (b) and (d), correspondingly

Hardness detection. The Vickers hardness values at the $(\overline{2}01)$ β-Ga$_2$O$_3$ samples surfaces were measured and calculated, they are: H_V (bulk face) = 8.80 ± 0.45 GPa; H_V (bulk back) = 9.25 ± 0.38 GPa. Considering the high anisotropy of the gallium oxide bulk crystal, the hardness values vary in a wide range. According to the majority of works [4,5,7,8,13] the hardness was measured at the (100), (010), (001) planes and is in the range of 8.3-12.8 GPa. We have found just one proceeding [18], where the hardness value was detected at the $(\overline{2}01)$ surface and amounted to H_V = 12.5 GPa. Overall, one can confirm that the H$_V$ values calculated in the present paper falls within the range indicated above.

Tribological test, friction force *(F_{fr})* **and coefficient of friction (COF)** *(μ)* **determination.** The amplitude of reciprocating motion in the experiments on friction of sapphire ball on crystal surfaces was 6 mm, the total length of the counterbody run was 50 m, the number of cycles was 4167, the maximum linear speed of the probe relative to the sample surface was 5.65 cm/s. The normal load (F_n) on the counterbody was 1 N. To increase the reliability of the results, the test was performed three times for any considered surface of each specimen.

The results of the tribotests are shown in Fig. 3. In addition to the change of F_{fr}, it shows the depth of the probe immersion (depth) depending on the change of its position coordinate during the test. The sharp increase of F_{fr} on the surface of the bulk face sample (Fig. 3(a)) beginning from about 22 m of the probe run attracts attention. Hence, beginning from about 30 m of the probe run the F_{fr} value stabilizes at the 0.085 N. At the same time the amplitude of friction force modulation increases. For the rear sample side (bulk back) which is the rougher one, the increase in F_{fr} is observed at the beginning of the test (Fig. 3(b)) and persists until the end, but with a less intensity. At the same time, the overall level of the amplitude of friction force modulation is high throughout the entire tribotest.
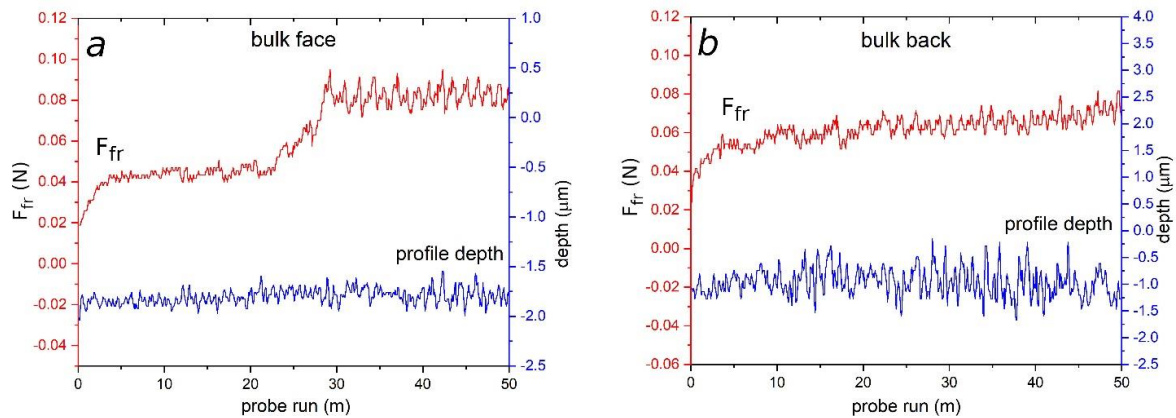

Fig. 3. The dependences of the friction force (F_{fr}) and probe immersion depth (depth) on the probe coordinate at the surfaces of the β-Ga_2O_3 sample: bulk face (a), bulk back (b)

The rise in the F_{fr} in the initial sections of the both tribotests may be related to the accumulation of wear particles in the friction zone [16,17]. The increased F_{fr} start-value for the bulk back sample experiment (0.04 *vs.* 0.02 N, see Fig. 3), as well as the higher overall level of the modulation amplitude can be explained by the higher initial surface roughness of this sample.

In our previous work [17] during a similar tribotest, but with a higher probe load value ($F_n = 2$ N), we encountered a situation in which the correctness of the test was not ensured due to the catastrophic destruction of the surface in the wear track. This fact did not allow us to obtain a legitimate COF value. It was concluded that the subsurface layers of the substrate, which had been undergone the post-growth processing, altered from the sample volume by a more defective structure containing interdomain boundaries. In other words, in the friction process, the sample acquires a mosaic structure. At $F_n = 1$ N the correctness of the tribological test is complied, since according to the change in the coordinate of immersion of the probe no total destruction of the surface is occurred. Nevertheless, the F_{fr} value (also COF) for the bulk face sample is an average, because the experiment actually consists of two parts yielding two significantly different F_{fr} values (also COF). At the same time, this value coincides with the value measured for the bulk back sample with the accuracy of the experimental error. Obviously, in case of the bulk back sample (Fig. 3(b)) more stable course of friction force is registered and the given F_{fr} values (also with COF) should be considered reliable. Proceeding

from the fact that the tribotest was carried out at $F_n = 1$ N, the values of COF and F_{fr} are equal in modulo.

The average COF values for the counterbodies involved in this tribotest are as follows: <μ> (bulk face sample) = 0.063 ± 0.019, <μ> (bulk back sample) = 0.062 ± 0.008. To the best of our knowledge, in 2020 an attempt to study the tribological characteristics of bulk gallium oxide crystals using the *nano scratch test* was made for the first time [29,30]. However, these publications did not provide a reliable value for the COF of this material. Later, in 2021, our group realized a reciprocating test to determine the μ values for quasi-bulk β-Ga₂O₃ 5-15 μm thick layers grown by the Halide Vapor Phase Epitaxy (HVPE) on sapphire substrates [16]. Those experiments performed under similar conditions show relatively similar results for a 5 μm thick layer (μ = 0.07) and different ones for a 15 μm thick layer (μ = 0.11). The discrepancy in COFs can be attributed to various degrees of crystalline perfection. The structure of the upper regions of the thicker heteroepitaxial layers is usually of higher crystallinity because of the greater distance from the interface. This is due to the reduced influence of the mismatch between the rhombohedral crystal system of the sapphire substrate and the monoclinic crystal system of the β-polymorph.

Finally, it should be noted that the COF values measured for the gallium oxide bulk crystals in this work, as well as for the gallium oxide layers in previous one are low, they are more than half the values obtained for sapphire [31].

XRD study. The first series of XRD measurements were performed for the initial samples. The θ-2θ curves are similar to those obtained on the samples subjected to the tribological experiment. Therefore, to save space, initial samples XRD patterns are not given in this paper.

The β-Ga₂O₃ diffraction pattern is shown in Fig. 4. It was measured in the θ-2θ mode for one of the samples after the tribotest. The most intense peaks at the pattern correspond to 5 orders of reflection in the [$\overline{2}$01] direction, from the $\overline{2}$01 itself up to the $\overline{10}$05. This XRD pattern confirms that the material of the sample corresponds to β-Ga₂O₃ (01-041-1103 in the ICDD file): a crystal of monoclinic system, $C2/m$ (12) group with lattice constants $a = 12.2270$ Å, $b = 3.0389$ Å, $c = 5.8079$ Å and $β = 103.82°$. Thus, the sample is a single-phase, it contains only the thermally stable β-modification, and the studied surface of the sample corresponds to the ($\overline{2}$01) plane.
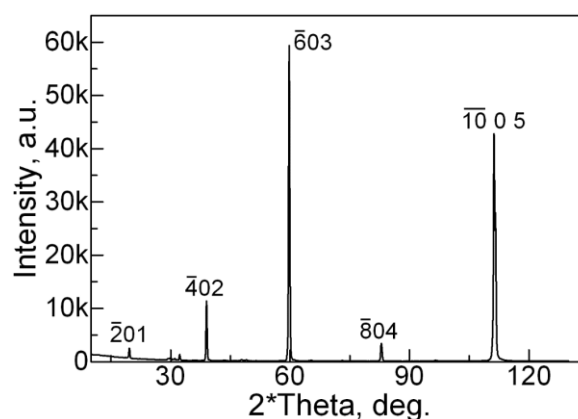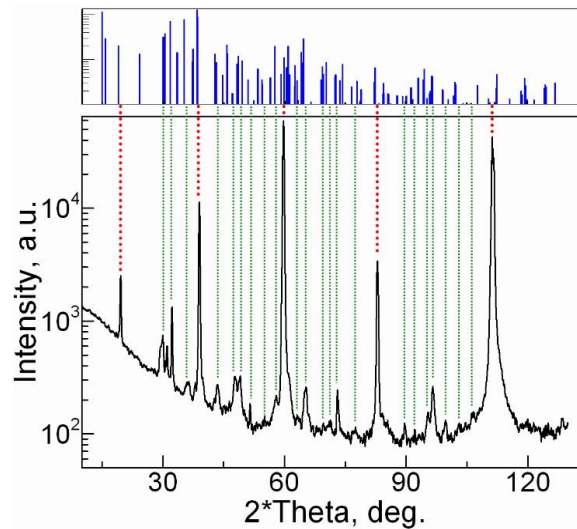

Fig. 4. The measured β-Ga₂O₃ diffraction pattern

Fig. 5. The β-Ga$_2$O$_3$ XRD pattern recorded in θ-2θ mode at Cu K$_{α1}$ radiation (the bottom part) in semilogarithmic scale. The upper part: the same, but the model X-ray powder diffraction pattern. The green dashed lines show the correspondence between the experimental and model reflections. The red dotted lines correspond to reflections that are multiples of the $\overline{2}01$ plane

The same diffraction curve (see Fig. 4) is depicted in semilogarithmic scale in the bottom part of the Fig. 5. The upper part of this figure shows a model X-ray powder diffraction pattern from β-Ga$_2$O$_3$ compiled from the data analysis of three ICDD files (00-041-1103, 01-074-1776, 01-087-1901). It can be seen that, in most cases, a possible correspondence among the model β-Ga$_2$O$_3$ reflection lines can be found for the low-intensity reflections that are presented on the measured diffraction curve. The exception are a few lines located in the region of relatively small 2θ angles (up to 30°). This fact may be an evidence of the presence of a powder fraction or polycrystalline component in the sample. The low intensity of the powder diffraction reflections shows that the powder fraction in the sample is relatively small. The powder particles were identified and analyzed in our previous study, in which a similar experiment was performed [17].

The reflections that correspond to 2θ angles scattering up to 30° are absent on the measured θ-2θ curve. This may be due to the fact that in this part of the diffraction pattern there is a rapidly falling background, which can prevent direct observation of attenuated reflections from a relatively small in volume powder fraction.

Wear coefficient (k) calculation. Both surfaces were examined using SEM to visualize and measure wear tracks widths (see Fig. 6). It is noteworthy to see more than a sixfold (105 *vs.* 650 μm, respectively) broadening of the wear track recorded at the bulk face sample surface. These data are consistent with the experimental results of the 3D wear tracks scanned by the profilometer. In Fig. 7 two such images of occasionally selected cross-sections perpendicular to the wear track are depicted. Based on calculation of these wear track areas and on assumption of averaging of the section geometry, the volumes of wear tracks were determined.

Then the wear coefficients were calculated (k = [mm^3/N·m]) according to the Archard model. The value of wear coefficient of the bulk face sample happened to be $(2.2 \pm 0.6)\ 10^{-2}$ mm^3/N·m. It should be noted that this is an extremely high indicator, corresponding to the values of soft steels. The reason for this fact may be significant changes in the structure of the single crystal due to the influence of post-growth processing. In [17], our tribological test was actually a simulation of post-growth processing of the substrate single crystal, due to which the latter acquired a mosaic structure. In contrast, the wear

coefficient measured on the opposite sample side (bulk back) has a rather low value $((1.1 \pm 0.1) \ 10^{-7} \ \text{mm}^3/\text{N·m})$. It is significantly lower than ones previously recorded for Ga$_2$O$_3$ β-polymorph 15 μm thick layers: $k = 5 \cdot 10^{-5} \ \text{mm}^3/\text{N·m}$ (100Cr6 steel counterbody) [15] and $k = (3.7 \pm 1.0) 10^{-4} \ \text{mm}^3/\text{N·m}$ (sapphire counterbody) [16].
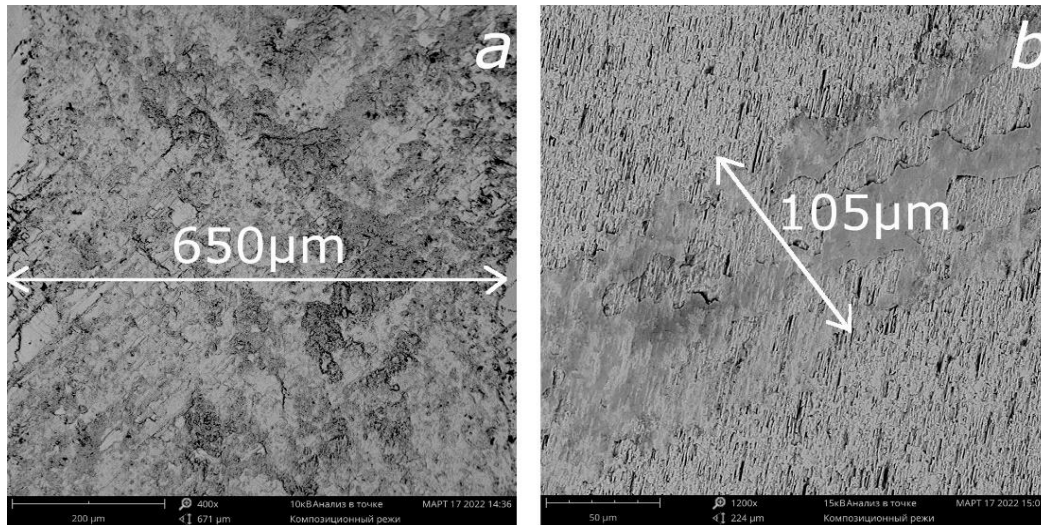

Fig. 6. SEM images of both the sample sides. The wear tracks upon the tribotest of the ($\bar{2}01$) β-Ga$_2$O$_3$ surface: bulk face (a), bulk back (b)
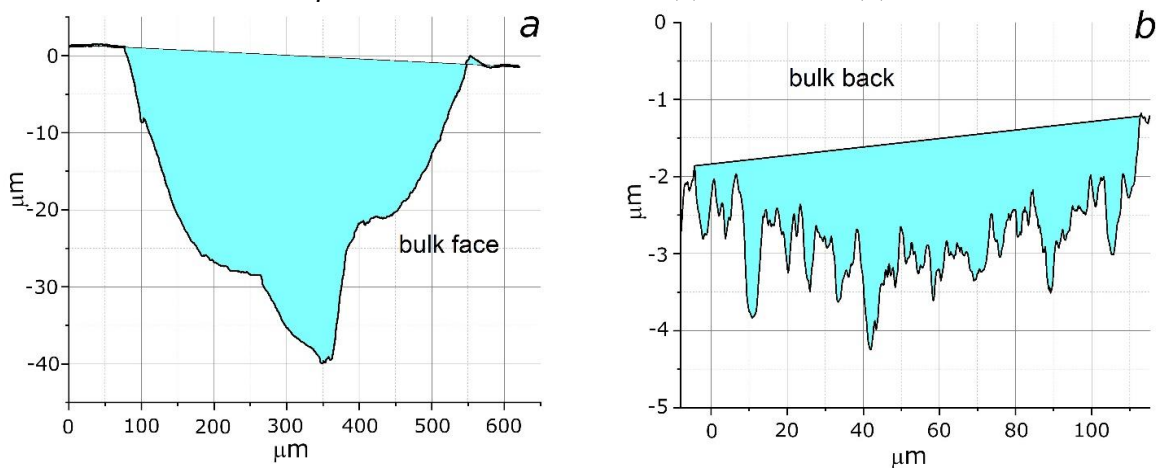

Fig. 7. Cross-sections of the wear tracks upon tribotest at β-Ga$_2$O$_3$ surface: bulk face (a), bulk back (b)

Figure 8 compares the COF (μ), wear coefficient (k) and hardness (H_V) values of the β-Ga$_2$O$_3$ samples: bulk face, bulk back and sapphire [32]. The bulk face sample has the lowest hardness and the highest wear coefficient. At the same time, the values of COFs of both sides of gallium oxide are low, almost 2 times lower than those of sapphire. Thus, the CMP-treated gallium oxide surface, i.e. the *epi-ready* surface, is the least perfect from the mechanical point of view.
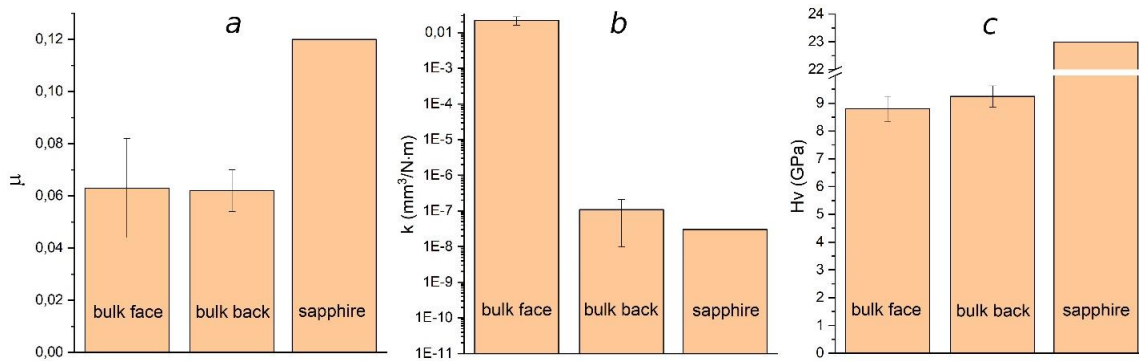
Fig. 8. Values of the COF (μ) (a), wear coefficient (k) (b) and hardness (H_V) (c) for the β-Ga$_2$O$_3$: bulk face, bulk back and sapphire. Based on [32]

Conclusions

The values of coefficient of dry friction (μ) and wear coefficient (k) of bulk ($\bar{2}01$) β-Ga$_2$O$_3$ single crystals used as *epi-ready* substrates were determined for the first time. The μ value is 0.063, which is significantly lower than the values for the currently used semiconductor materials. At the same time, the k values for the surface prepared (post-growth processing) by polishing and chemical-mechanical polishing (CMP) differ significantly: $1.1 \cdot 10^{-7}$ and $2.2 \cdot 10^{-2}$ mm^3/N·m, correspondingly.

The hardness (H_V) of bulk gallium oxide crystals measured at the ($\bar{2}01$) plane is relatively high (9 GPa), but it is more than half that of sapphire. Moreover, the hardness of the CMP polished substrates is slightly lower than that one measured on the polished surface. It is noteworthy that the lower H_V value of gallium oxide corresponds to its lower μ values.

An important result obtained in this study is the fact that the smoother *epi-ready* surface of gallium oxide semiconductor substrates happens to have lower mechanical parameters (tribological characteristics and hardness) compared to not completely post-growth-processed surface. The reason for this fact is that the structure of the *epi-ready* substrates might contain a large number of unrelaxed stresses in the subsurface layers due to the influence of deformation defects that were input during full-cycle post-growth processing. Thus, from the point of view of mechanical properties, the bulk β-Ga$_2$O$_3$ substrate crystals grown by the EFG are undoubtedly promising materials, however, it is obvious that their preparation for epitaxial growth processes should be studied more deeply.

References

1. Stepanov S, Nikolaev V, Bougrov V, Romanov A. Gallium OXIDE: Properties and application: a review. *Rev. Adv. Mater. Sci.* 2016;44(1): 63–86.
2. Higashiwaki M. β-Ga$_2$O$_3$ material properties, growth technologies, and devices: A Review. *AAPPS Bulletin*. 2022;32: 3.
3. Goto K, Murakami H, Kuramata A, Yamakoshi S, Higashiwaki M, Kumagai Y. Effect of substrate orientation on homoepitaxial growth of β-Ga$_2$O$_3$ by halide vapor phase epitaxy. *Applied Physics Letters*. 2022;120(10): 102102.
4. Huang H, Li X, Mu D, Lawn BR. Science and art of ductile grinding of brittle solids. *International Journal of Machine Tools and Manufacture*. 2021;161: 103675.
5. Xu YM, Zhou H, Zhang JQ, Ren XP, Zhang CW. Experimental study on microscale mechanical behavior of easily cleavable gallium oxide crystals. *China Mech. Eng.* 2022;33(18): 27823-27835.
6. Wu YQ, Gao S, Huang H. The deformation pattern of single crystal β-Ga$_2$O$_3$ under nanoindentation. *Materials Science in Semiconductor Processing*. 2017;71: 321–325.

7. Zhang JQ, Zhou H, Jiang W, Hu SX, Ren XP, Zhang CW. Investigation of dynamic mechanical properties and constitutive model of (010) plane of gallium oxide crystals under shock loading. *Ceramics International*. 2022;48(19): 27823–27835.

8. Mu W, Jia Z, Yin Y, Hu Q, Li Y, Wu B. High quality crystal growth and anisotropic physical characterization of β-Ga₂O₃ single crystals grown by EFG Method. *Journal of Alloys and Compounds*. 2017;714: 453–458.

9. Gao S, Wu Y, Kang R, Huang H. Nanogrinding induced surface and deformation mechanism of single crystal β-Ga₂O₃. *Materials Science in Semiconductor Processing*. 2018;79: 165–170.

10. Gao P, Tan B, Yang F, Li H, Bian N, Sun X. Influence of diamond wire saw slicing parameters on (010) lattice plane beta-gallium oxide single crystal wafer. *Materials Science in Semiconductor Processing*. 2021;133: 105939.

11. Grashchenko AS, Kukushkin SA, Osipov AV, Red'kov AV. Investigation of the physicomechanical characteristics of nanoscale films by nanoindentation. *Mechanics of Solids*. 2018;53(5): 481–488.

12. Battu AK, Ramana CV. Mechanical properties of nanocrystalline and amorphous gallium oxide thin films. *Advanced Engineering Materials*. 2018;20(11): 1701033.

13. Zhou H, Wei J, Shen J, Xu Y, Zhang J. Study on the size effect of single crystal gallium oxide during the nanoindentation process. *Journal of Advanced Manufacturing Systems*. 2021;20(03): 575–587.

14. Wu YQ, Gao S, Kang RK, Huang H. Deformation patterns and fracture stress of beta-phase gallium oxide single crystal obtained using compression of micro-pillars. *Journal of Materials Science*. 2018;54(3): 1958–1966.

15. Butenko PN, Guzilova LI, Chikiryaka AV, Pechnikov AI, Grashchenko AS, Pozdnyakov AO, Nikolaev VI. Wear resistance of α-and β-gallium oxide coatings. *Materials Physics and Mechanics*. 2021;47(1): 52-58.

16. Butenko PN, Guzilova LI, Chikiryaka AV, Pechnikov AI, Nikolaev VI. Tribological Studies of α-β-Ga₂O₃ Layers Paired with a Sapphire Counterface. *Technical Physics*. 2021;66: 1186–1193.

17. Butenko PN, Guzilova LI, Chikiryaka AV, Boiko ME, Sharkov MD, Almaev AV. Impact on the subsurface layers of the single-crystal β-Ga₂O₃ wafers induced by a mechanical wear. *Materials Science in Semiconductor Processing*. 2022;143: 106520.

18. Víllora EG, Arjoca S, Shimamura K, Inomata D, Aoki K. β-Ga₂O₃ and single-crystal phosphors for high-brightness white LEDs and LDs, and β-Ga₂O₃ potential for next generation of power devices. *SPIE Proceedings*. 2014;8987: 371-338.

19. Blevins JD, Stevens K, Lindsey A, Foundos G, Sande L. Development of large diameter semi-insulating gallium oxide (Ga₂O₃) substrates. *IEEE Transactions on Semiconductor Manufacturing*. 2019;32(4): 466–472.

20. Galazka Z, Ganschow S, Seyidov P, Irmscher K, Pietsch M, Chou T-S. Two inch diameter, highly conducting bulk β-Ga₂O₃ single crystals grown by the Czochralski method. *Applied Physics Letters*. 2022;120(15): 152101.

21. Itoh T, Mauze A, Zhang Y, Speck JS. Epitaxial growth of β-Ga₂O₃ on (110) substrate by plasma-assisted molecular beam epitaxy. *Applied Physics Letters*. 2020;117(15): 152105.

22. Cheng Y, Xu Y, Li Z, Zhang J, Chen D, Feng Q. Heteroepitaxial growth of α-Ga₂O₃ thin films on a-, C- and R-plane sapphire substrates by low-cost mist-CVD method. *Journal of Alloys and Compounds*. 2020;831: 154776.

23. Biswas M, Nishinaka H. Thermodynamically metastable α-, ε- (or κ-), and γ-ga2o3: From material growth to device applications. *APL Materials*. 2022;10(6): 060701.

24. Nikolic MV, Milovanovic V, Vasiljevic ZZ, Stamenkovic Z. Semiconductor gas sensors: Materials, technology, design, and application. *Sensors*. 2020;20(22): 6694.

25. Almaev A, Nikolaev V, Butenko P, Stepanov S, Pechnikov A, Yakovlev N. Gas sensors based on pseudohexagonal phase of gallium oxide. *Physica Status Solidi (b)*. 2021;259(2): 2100306.

26. Yakovlev N, Almaev A, Butenko P, Tetelbaum D, Mikhaylov A, Nikolskaya A. Effect of Si+ ion implantation in α-Ga$_2$O$_3$ films on their gas sensitivity. *IEEE Sensors Journal*. 2023;23(3): 1885–1895.

27. Ma X, Xu R, Xu J, Ying L, Mei Y, Long H. In-plane crystalline anisotropy of bulk β-Ga$_2$O$_3$. *Journal of Applied Crystallography*. 2021;54(4): 1153–1157.

28. Archard J. Contact and rubbing of flat surfaces. *Journal of Applied Physics*. 1953;24(8): 981-988.

29. Zhou H, Xu Y, Zhang J, Shen J, Huang M. Effect of scratching speed on the brittle-plastic transition of single crystal gallium oxide. In: *2020 6th International Conference on Mechanical Engineering and Automation Science (ICMEAS)*. 2020. p.247–253.

30. Zhou H, Song F, Wei JH. Nanomechanical Properties of β-Ga$_2$O$_3$ with different Crystal Planes. *Journal of the Chinese Ceramic Society*. 2020;48(1): 135–139.

31. Zeng G, Tan C-K, Tansu N, Krick BA. Ultralow wear of gallium nitride. *Applied Physics Letters*. 2016;109(5): 051602.

32. Alisin V. Tribological properties of sapphire under dry friction against chromium and zirconium ceramics. *Materials Research Proceedings*. 2022;21: 18.

THE AUTHORS

Butenko P.N.
e-mail: pavel@butenko.info

Boiko M.E.
e-mail: M.E.Boiko@mail.ioffe.ru

Chikiryaka A.V.
e-mail: chikiryaka@mail.ru

Guzilova L.I.
e-mail: guzilova@mail.ioffe.ru

Pozdnyakov A.O.
e-mail: ao.pozd@mail.ioffe.ru

Sharkov M.D.
e-mail: mischar@mail.ru

Almaev A.V.
e-mail: almaev_alex@mail.ru

Nikolaev V.I.
e-mail: nikolaev.v@mail.ioffe.ru